Molecular Plant • Volume 7 • Number 1 • Pages 137–155 • January 2014 RESEARCH ARTICLE

Arabidopsis Coordinates the Diurnal Regulation of Carbon Allocation and Growth across a Wide Range of Photoperiods

Ronan Sulpice[a,b,2], Anna Flis[a,2], Alexander A. Ivakov[a], Federico Apelt[a], Nicole Krohn[a], Beatrice Encke[a], Christin Abel[a], Regina Feil[a], John E. Lunn[a], and **Mark Stitt[a,1]**

a Max Planck Institute of Molecular Plant Physiology, Am Muehlenberg 1, 14476 Potsdam-Golm, Germany
b Present address: National University of Galway, Plant Systems Biology Lab, Plant and AgriBiosciences Research Centre, Botany and Plant Science, Galway, Ireland

ABSTRACT In short photoperiods, plants accumulate starch more rapidly in the light and degrade it more slowly at night, ensuring that their starch reserves last until dawn. To investigate the accompanying changes in the timing of growth, *Arabidopsis* was grown in a range of photoperiods and analyzed for rosette biomass, photosynthesis, respiration, ribosome abundance, polysome loading, starch, and over 40 metabolites at dawn and dusk. The data set was used to model growth rates in the daytime and night, and to identify metabolites that correlate with growth. Modeled growth rates and polysome loading were high in the daytime and at night in long photoperiods, but decreased at night in short photoperiods. Ribosome abundance was similar in all photoperiods. It is discussed how the amount of starch accumulated in the light period, the length of the night, and maintenance costs interact to constrain growth at night in short photoperiods, and alter the strategy for optimizing ribosome use. Significant correlations were found in the daytime and the night between growth rates and the levels of the sugar-signal trehalose 6-phosphate and the amino acid biosynthesis intermediate shikimate, identifying these metabolites as hubs in a network that coordinates growth with diurnal changes in the carbon supply.

Key words: *Arabidopsis*; diurnal; growth; photoperiod; ribosomes; trehalose-6-phosphate; starch.

INTRODUCTION

In the light, photosynthesis provides energy and carbon (C) for growth, whilst, at night, metabolism and growth depend on C reserves that accumulated in preceding light periods. Many plants use starch as their major transient C reserve. Starch is accumulated in the light and remobilized at night to support metabolism and growth (Zeeman et al., 2010). Starch is degraded in a near-linear manner such that starch is almost but not completely exhausted at dawn (Geiger and Servaites, 1994; Graf et al., 2010; Stitt and Zeeman, 2012). This maximizes growth by ensuring that almost all of the newly fixed C is immediately invested in growth, while minimizing the risk of C starvation at the end of the night (Rasse and Tocquin, 2006; Graf et al., 2010; Stitt and Zeeman, 2012).

This pattern of starch turnover is remarkably robust against changes in the environment. When less C is available (e.g. short days, low light), a larger proportion of the photosynthate accumulates as starch in the light and starch is degraded more slowly during the night (Chatterton and Silvius, 1979, 1980; Smith and Stitt, 2007; Stitt et al., 2007a). It was recently shown that starch degradation adjusts almost immediately to sudden changes in the light regime (Lu et al., 2005; Graf et al., 2010) and temperature (Pyl et al., 2012). This allows plants to exquisitely pace the use of their C reserves in a fluctuating environment.

The circadian clock facilitates predictive, temporal regulation of molecular and physiological processes over the 24-h day/night cycle (Troein et al., 2009; Farre and Weise, 2012; Chow and Kay, 2013). It was recently shown that the clock regulates starch breakdown (Graf et al., 2010). In the short period *lhycca1* clock mutant, starch was exhausted about 20 h after the previous dawn (i.e. ZT20), coinciding with the rise of dawn marker transcripts. When wild-type plants were grown in an 18.5- or a 28-h T-cycle, they still exhausted their starch ~24 h after the previous dawn; consequently, starch was not fully mobilized in a T-18.5 cycle, whereas it was depleted

[1] To whom correspondence should be addressed. E-mail mstitt@mpimp-golm.mpg.de, tel. +49 331 567 8100, fax +49 331 567 8101.

[2] These two authors contributed equally to this paper.

doi:10.1093/mp/sst127, Advance Access publication 11 October 2013

Received 26 July 2013; accepted 20 August 2013

about 4 h before dawn in a T-28 cycle. These results led to the proposal that starch degradation is timed such that starch is exhausted at dawn as anticipated by the clock (Graf et al., 2010; Graf and Smith, 2011; Scialdone et al., 2013). This provides a framework to understand how starch breakdown is adjusted to long-term differences in growth photoperiod and to sudden changes in the light regime or the night temperature (Graf et al., 2010; Graf and Smith, 2011; Pyl et al., 2012; Stitt and Zeeman, 2012). The mechanism whereby the clock paces starch breakdown is unknown. It presumably requires measurement of the amount of starch and of the time to dawn, and integration of this information to set an appropriate rate of starch breakdown (Graf and Smith, 2011; Scialdone et al., 2013).

Starch synthesis is regulated by ADP glucose pyrophosphorylase (AGPase) (Stitt et al., 2010; Zeeman et al., 2010; Hadrich et al., 2012). AGPase is allosterically activated by a rising glycerate-3-phosphate/Pi ratio. This acts to stimulate starch synthesis when the rate of photosynthesis exceeds the rate at which triose-phosphate is exported from the chloroplast and used to synthesize sucrose and other end products (Stitt et al., 2010). AGPase is also subject to posttranslational redox regulation (Tiessen et al., 2002; Hendriks et al., 2003). Activation occurs in response to light and sugar. Activation by sugars is mediated by NADP-thioredoxin reductase C (NTRC) (Michalska et al., 2009; Barajas-Lopez et al., 2011), and correlates with changes in the sucrose-signal trehalose 6-phosphate (Tre6P) (Kolbe et al., 2005; Lunn et al., 2006). Allosteric and posttranslational regulation will act to stimulate starch synthesis when there is a momentary excess of photosynthate or sucrose (Stitt et al., 2010). However, they do not readily explain how starch synthesis is regulated to provide an appropriate amount of C reserve for the night, especially in short days when less C is available. It is also unclear whether starch synthesis is regulated by the clock.

The pattern of starch turnover has consequences for the diurnal timing and efficiency of growth (Stitt and Zeeman, 2012). Starchless mutants grow like wild-type plants in long-day conditions, but are unable to grow in short days (Caspar et al., 1985; Gibon et al., 2004). They exhaust their C reserves in the first hours of the night, and this is followed by transcriptional activation of C-starvation responses, an increase of metabolites that derive from degradation of proteins, cell walls, and lipids, and an inhibition of growth that is not reversed until several hours into the following light period (Gibon et al., 2004; Blasing et al., 2005; Usadel et al., 2008; Yazdanbakhsh et al., 2011). Small disturbances of starch turnover also impair growth. Time-resolved measurements of root growth showed that growth in the *lhycca1* resembles wild-type *Arabidopsis* over much of the 24-h cycle but is inhibited towards the end of the night, when starch is exhausted. This inhibition can be reversed by adding sucrose (Yazdanbakhsh et al., 2011). On the other hand, if consumption of C for growth were to exceed the rate of C release from starch, this would result in depletion of sugars and C-starvation, even though the plant conserves starch until dawn.

In a previous study with *Arabidopsis*, we reported a progressive stimulation of starch synthesis and inhibition of starch degradation as the photoperiod was decreased from 12 to 2 h (Gibon et al., 2009). However, there was only a small decrease in sucrose levels at the end of the night, implying that there is coordinate regulation of starch degradation and growth (Gibon et al., 2009). Profiling of enzyme activities revealed capacity for photosynthesis was maintained whilst capacity for metabolic pathways required in growth was decreased. The following experiments extend these earlier studies. By combining information about diurnal changes of starch and metabolites with measurements of photosynthesis and respiration, we model the rate of growth in the light period and the night. We then use metabolite profiling to identify metabolites that correlate with the rate of growth.

RESULTS

Biomass, Relative Growth Rate, and C Conversion Efficiency

Wild-type *Arabidopsis* Col0 was grown in a 18-h/6-h, 12-h/12-h, 8-h/16-h, 6-h/18-h, and 4-h/20-h light/dark cycle. Whole rosettes of 29-day-old plants were harvested at the end of the night (EN) and the end of the day (ED) and analyzed for fresh weight (FW), dry weight (DW), and metabolites using robotized platforms and LC–MS/MS. Whole rosette photosynthesis was measured in the middle of the day and respiration towards the EN. The data are summarized in Supplemental Table 1.

Lengthening the photoperiod resulted in an increase in rosette FW (Figure 1A). Relative growth rate (RGR) calculated on a FW basis increased in a near-liner manner as the photoperiod increased from 4 to 12 h, but showed only a small further increase in the 18-h photoperiod (Figure 1B). Protein content did not change, chlorophyll a and chlorophyll b rose by about 20% between a 4- and 12-h photoperiod, and the chlorophyll a/b ratio rose from 3.5 to 4.2 (Supplemental Table 1 and Supplemental Figure 1). The DW content (DWC) was about 8% in the 6-, 8-, 12-, and 18-h photoperiod treatments (Supplemental Figure 1A and Supplemental Table 1). DWC was consistently higher at ED than at EN (8.94–9.14% and 7.45–7.97%, respectively); this may be partly due to lower leaf water content due to transpiration in the light and partly to accumulation of starch and other metabolites in the light period (see below). DW content could not be determined for the 4-h photoperiod samples due to lack of material; however, the similar protein content in all photoperiods indicates that DW content in the 4-h photoperiod probably resembles that in longer photoperiods. The impact of photoperiod on RGR on a DW basis resembles that on a FW basis (Figure 1B).

Photosynthesis, Respiration, Net Daily C Gain, and Growth per 24-h Cycle

The rate of photosynthesis (A, μmol CO_2 g^{-1} FW h^{-1}) was similar in the 4-, 6-, 8-, and 12-h photoperiods, and decreased in

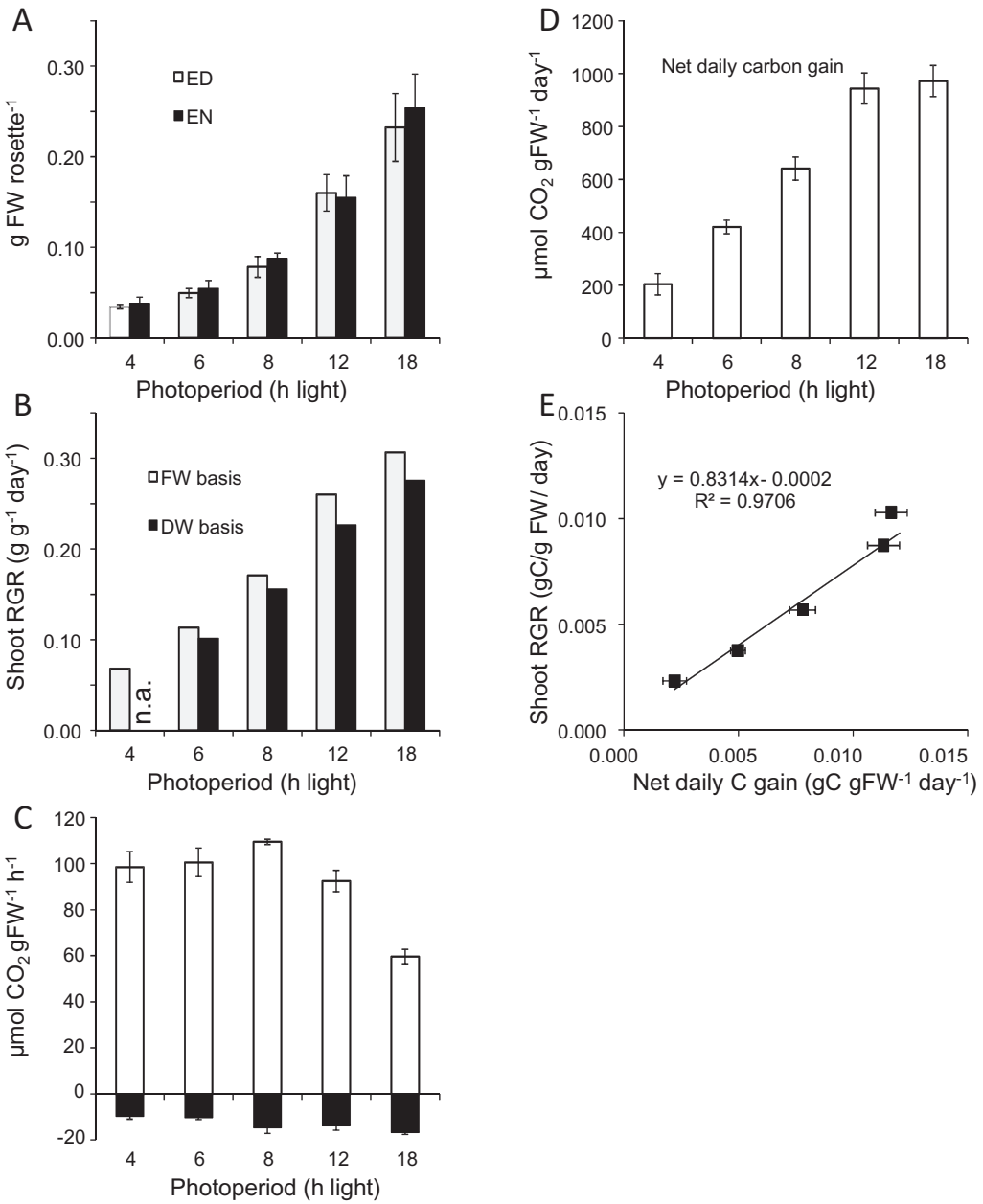

Figure 1. Biomass and Structural Components.

(A) Rosette biomass (FW).

(B) RGR, calculated from the incremental increased in rosette biomass.

(C) Photosynthesis and respiration.

(D) Net carbon gain per 24-h period calculated as [(A × hours light) – (R × hours darkness)] where A = µmol CO_2 fixed g FW h^{-1}, and R = µmol CO_2 respired g FW h^{-1}.

(E) Net carbon gain per 24 h plotted against the daily gain in C in biomass. The latter is calculated as RGR (g FW d^{-1}) × DWC/100 × 0.4 (see Supplemental Table 1), where 0.4 is the mass contribution of C to plant DW. Source data are provided in Supplemental Table 1. The results are the mean ± SD (n ≥ 5). n.a., not available.

the 18-h photoperiod (Figure 1C). The rate of respiration (R µmol CO_2 g^{-1} FW h^{-1}) rose two-fold between short and long photoperiods (Figure 1C). Net daily C gain (Figure 1D) was calculated by subtracting summed respiration per day (R^D) from summed photosynthesis per day (A^D). It increased in a linear manner between the 4- and 12-h photoperiods, but only increased slightly between the 12- and 18-h photoperiod. The intercept on the *x*-axis at ~2 h matches the photoperiod at which *Arabidopsis* is unable to grow (Gibon et al., 2009). A plot of net daily C gain against RGR yielded a straight line, with an intercept close to zero and a slope of 0.83 (Figure 1E). This reveals that C-conversion efficiency is similar across this

wide range of photoperiods. About 80% of the net fixed C is recovered in rosette biomass, and the remainder is probably in root biomass or exuded into the soil. The agreement between growth rate estimated from biomass accumulation and growth rate estimated from gas exchange documents the reliability of our analyses.

The correlation between photoperiod length and growth breaks down at longer photoperiods (Figure 1D). One reason is the decrease in photosynthesis per unit FW in the 18-h photoperiod. This was not due to a decrease in total protein or chlorophyll content per unit FW (Supplemental Figure 1). Leaf morphology was analyzed in a separate experiment (Supplemental Figure 1). Leaf thickness increased between a 12-, 16-, and 22-h photoperiod. This will decrease the amount of new leaf area that is generated per unit of C invested and, consequently, attenuate the rate of growth (see the 'Discussion' section).

Starch, Sugars, and Total Amino Acids at EN and ED

Starch, sucrose, reducing sugars, malate and fumarate, and total amino acids were analyzed at EN and ED (Figure 2 and Supplemental Table 1). Starch levels at ED increased as the photoperiod was increased from 4 to 8 h, and then stabilized (Figure 2A; see also Gibon et al., 2009). Starch levels at EN were low in 4-, 6-, 8-, and 12-h photoperiods, but substantial in the 18-h photoperiod (equivalent to 11%, 12%, 10%, 15%, and 41% of starch at ED, respectively). The average rates of starch synthesis and degradation were estimated as the difference between starch at ED and EN, divided by the length of the light period, or the night, respectively. The average rate of starch synthesis decreased over three-fold between the 4- and 18-h photoperiods, with the largest decrease occurring at photoperiods above 8 h. Comparison with A (Figure 1C) reveals that 49%, 51%, 41%, 33%, and 24% of fixed C is allocated to starch in a 4-, 6-, 8-, 12-, and 18-h photoperiod, respectively. The average rate of starch degradation rose continuously as the photoperiod was lengthened. Comparison with the R (Figure 1C) reveals that about 100%, 59%, 64%, 45%, and 40% of the mobilized starch is respired in a 4-, 6-, 8-, 12-, and 18-h photoperiod, respectively.

Taken together, these data indicate that the rate of starch synthesis reaches an upper limit when starch synthesis consumes about half the fixed C. This value is reached when the photoperiod is decreased to 8 h. In shorter photoperiods, the starch content at ED decreases and the plants enter an increasingly long night with less starch, resulting in a strong decrease in the rate of starch degradation in short photoperiods.

Sucrose levels showed a progressive decrease at EN and ED as the photoperiod was decreased (Figure 2C). Sucrose was lower at EN than ED, and this difference became more marked in short photoperiods. Glucose levels at EN were strongly decreased in short photoperiods, but remained high in long photoperiods (Figure 2D). Amino acids showed a progressive decrease at EN and ED as the photoperiod was decreased, and were higher at ED than EN (Figure 2E). The absolute amount of C that accumulates in sugars and other soluble metabolites like organic acids and amino acids (see Supplemental Table 1) is much less than the amount that accumulates in starch (see also Gibon et al., 2009; Pyl et al., 2012).

C-Balance Model to Estimate Average Rates of Growth in the Light Period and Night

A C-balance model was used to estimate average rates of growth in the daytime and night. Growth in the light can be estimated as total photosynthesis per day minus the C that accumulates in starch and other metabolites (= $A^D - \Delta C$), and growth at night can be estimated as C mobilization out of starch and other metabolites minus respiration (= $\Delta C - R^D$). ΔC was estimated by summing C in starch, sugars, malate, fumarate, and total amino acids; about 80% was due to starch in all photoperiods (Table 1 and Supplemental Table 2). ΔC increased as the photoperiod was increased from 4 to 8 h, decreased slightly in the 12-h, and decreased markedly in the 18-h photoperiod. ΔC accounted for 66% of A^D in short days, falling to 30% in long days (Table 1). ΔC is similar to the parameter 'non-structural carbohydrates'. However, it additionally includes C accumulated in organic acids and amino acids, resulting in a small upward correction of the C that is transiently accumulated in starch and low-molecular-weight carbohydrates.

Figure 3A shows the modeled distribution of growth between the daytime and night (increase in biomass per light period or per night, μmol C g^{-1} FW h^{-1}). In very short days, almost all of the growth occurred in the light. In a 6-h photoperiod, half the growth occurred in the light and half at night. When photoperiod was further lengthened, an increasing proportion of the growth occurred in the daytime and growth in the night remained constant or (18 h) decreased slightly. Figure 3B shows the rates of growth (μmol C g^{-1} FW h^{-1}). The rate of growth in the daytime increased progressively as the photoperiod was lengthened. The lower rate in the light in short photoperiods reflects the increased allocation of fixed C to reserves. The decrease in the 18-h photoperiod is due to the lower rate of photosynthesis (see the 'Discussion' section). The rate of growth at night increased progressively as the photoperiod was lengthened. This reflects the fact that the plants have similar or slightly more C-reserves to support growth in an increasingly shorter night. In the 18-h photoperiod, the rate of growth in the night is similar to that in the day.

Respiration can be subdivided into growth respiration (R_g) and maintenance respiration (R_m) (Penning de Vries et al., 1974; Penning de Vries, 1975; Amthor, 2000). R*g* is the CO_2 released during the biosynthesis of new biomass, whilst R_m includes costs associated with turnover of cellular components and preservation of cellular function (e.g. pH and ionic gradients). R*g* was estimated (Table 1; see Supplemental Table 2 for calculation) using a typical value of 0.2 CO_2 released per unit C deposited in biomass (Penning de Vries et al., 1979). R*m* was estimated as (R–R*g*). R*g* increased with photoperiod, and R*m*

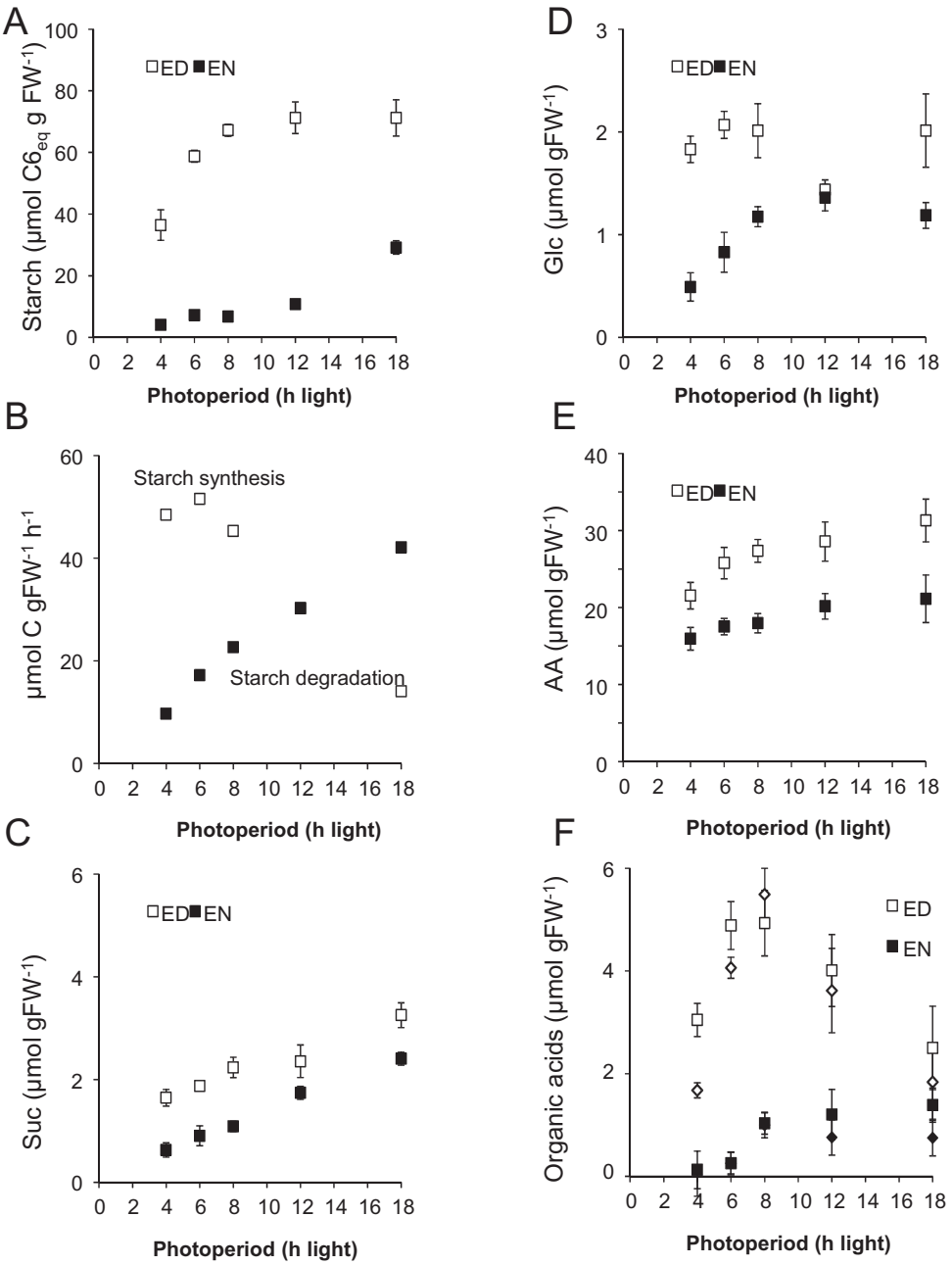

Figure 2. Starch, Sugars, Malate, Fumarate, and Total Amino Acids at EN and ED.

(A) Starch.
(B) Rates of starch synthesis and degradation.
(C) Sucrose.
(D) Glucose.
(E) Total amino acids.
(F) Malate (squares) and fumarate (diamonds). Data for ED and EN are shown separately. The data are provided in Supplemental Table 1. The results are the mean ± SD ($N \geq 5$).

was similar across all photoperiods (Table 1). R*m* accounted for 20% of the remobilized C in long photoperiods, and almost all the remobilized C at night in a 4-h photoperiod.

Our C-balance model defines growth as the conversion of C to structural components. Previous analyses of diurnal growth patterns analyzed temporal sequences of 2-D images to provide information about the timing of leaf expansion (Wiese et al., 2007; Walter et al., 2009; Poire et al., 2010). Leaf expansion is mainly due to cell expansion driven by water uptake. We analyzed leaf area images collected at EN and

Table 1. Diurnal C Balance.

Photo period	ΔC	Rate of ΔC mobilization	R_g	R_m	$\Delta C/A^D$	$R^D/\Delta C$
	μmol C g^{-1} FW h^{-1}	μmol C g^{-1} FW h^{-1}	μmol C g^{-1} FW h^{-1}	μmol C g^{-1} FW h^{-1}	%	%
4 h	259	12.9	0.6	9.1	65.7	70
6 h	397	23.0	2.4	7.5	65.8	39
8 h	454	28.4	2.8	11.9	51.9	45
12 h	428	35.6	4.4	9.3	38.6	26
18 h	320	53.4	7.3	9.4	29.8	18

C in major metabolite pools was summed at ED and EN, and the difference subtracted to estimate the diurnal turnover of C (ΔC). The following metabolites were used in this calculation: starch, sucrose, glucose, fructose, malate, fumarate, and total amino acids (assuming an average of 2.8 C per amino acid). The calculation was performed for the experiment of Figures 1 and 2, source data are provided in Supplemental Table 1, and an extended version of the calculation is provided in Supplemental Table 2.

ED on three consecutive days to estimate the average rate of rosette expansion in the light and dark (Figure 3C). In a 12-h photoperiod, the rate of rosette expansion was slightly higher in the light than the dark. This difference became much more marked in a 4-h photoperiod, confirming the results from the C-balance model. Comparison of Figure 3A and 3C indicates that analyses of expansion growth may slightly underestimate growth (defined as conversion of C to structural biomass) in the light and overestimate growth in the night.

Summarizing, growth is distributed flexibly between the daytime and night. In long photoperiods, growth rates in the night are as high as those in the daytime. As the photoperiod becomes shorter, growth at night is increasingly restricted by the size of the C reserve accumulated in the preceding light period. The amount of growth per night nevertheless rises as the night becomes longer, and is highest in a 6-h photoperiod.

Polysome Loading

Protein synthesis represents a major component of cellular growth (Warner, 1999; Rudra and Warner, 2004). The rate of protein synthesis depends on ribosome abundance and the loading of ribosomes into polysomes. To provide independent evidence for our estimates of the distribution of growth between the daytime and night in different photoperiods, we analyzed polysome loading and ribosome abundance at EN and ED (Figure 4).

Polysome loading was monitored using density gradient centrifugation (Bailey-Serres, 1999). Polysome loading remained high at night in a 12- and 18-h photoperiod but decreased in the night in short photoperiods (Figure 4A). This is qualitatively in agreement with our C-balance model (Figure 3B). It should be noted that the decrease in polysome loading at night underestimates the actual decrease in the rate of protein synthesis (Pal et al., 2013, see the 'Discussion' section).

Ribosome abundance was estimated from the total A_{254} signal. This signal agrees with the abundance of rRNA species, determined by quantitative qRT–PCR against the cytosolic, plastidic, and mitochondrial rRNA species (Piques et al., 2009; Pal et al., 2013). The A_{254} signal did not change between EN and ED (see also Pal et al., 2013) and did not change markedly between different photoperiods (Figure 4B). This was rather unexpected, as growth is much slower in short days than long days (see the 'Discussion' section).

Temporal Kinetics of Starch and Other Metabolites

The experiment of Figures 1–4 provides information about the average rates of starch synthesis, starch degradation, and growth in the daytime and night. A complementary experiment was performed in which plants were harvested at 2-h intervals through the diurnal cycle (Figure 5; see also Supplemental Table 3). This experiment was carried out with younger plants (21 d after germination). The levels of starch at ED and EN (Figure 5A) and the fraction of starch remaining at EN (12%, 12%, 10%, 14%, and 44% in a 4-, 6-, 8-, 12-, and 18-h photoperiods (calculated from Figure 5A) were similar to those in Figure 2. Whilst starch at ED was similar in the 12- and 18-h photoperiods in the experiment of Figure 2, it declined in the experiment of Figure 5. However, in both experiments, the rate of starch synthesis was much lower in an 18-h photoperiod than a 12-h photoperiod

The temporal kinetics of starch accumulation depended on the photoperiod (Figure 5A). First, whereas in short photoperiods starch accumulated in a near-linear manner after illumination, in the 18-h photoperiod, there was a very marked lag before starch started to accumulate. Closer inspection indicates that there may also be slight lag in the 6-, 8-, and 12-h photoperiods. This was confirmed for the 12-h photoperiod in a separate experiment (data not shown). A slight delay after the onset of illumination in the morning might be expected because it takes 10–15 min to reach full rates of photosynthesis. However, the large delay in the 18-h photoperiod cannot be explained in this manner. Second, whereas starch accumulation continues until ED in short photoperiods, it slows down in the last part of the light period in long photoperiods. This was noticeable in the 12-h photoperiod and marked in the 18-h photoperiod (see also Hadrich et al., 2012).

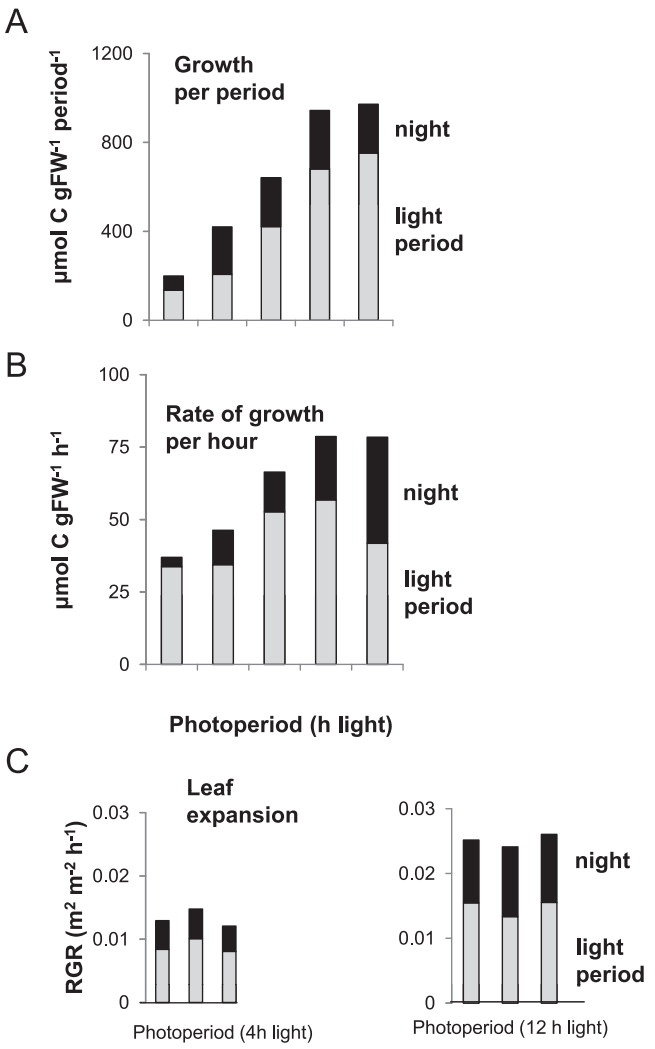

Figure 3. Distribution of Growth between the Daytime and the Night.
(A) Increment per period.
(B) Rate per hour. Growth in the daytime is estimated as total C fixed minus C accumulated in starch and metabolites (µmol C g^{-1} FW h^{-1}) and growth at night is calculated as C remobilized from starch and metabolites minus the total C respired (µmol C g^{-1} FW h^{-1}). The source data are provided in Supplemental Table 1 and the calculations in Supplemental Table 2.
(C) Leaf expansion rate in a 4- and 12-h photoperiod, estimated from the change in leaf area on three consecutive days, each shown separately.

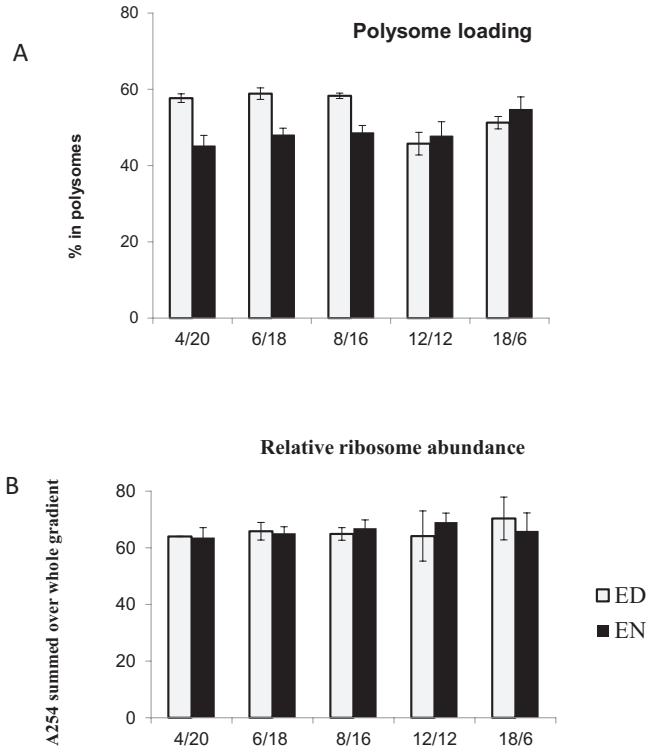

Figure 4. Polysome Loading and Ribosome Abundance.
(A) Polysome loading was monitored by analysis of polysome loading using density gradient centrifugation. rRNA constitutes the vast majority of the RNA in a cell, allowing the distribution of ribosomes to be assessed by monitoring absorption at 254 nm (A_{254}) in different fractions from the gradient. The gradient was divided into fractions corresponding to free ribosomes and monosomes (non-polysome fraction, NPS), small polysomes with fewer than five ribosomes (small polysome fraction, SPS) and large polysomes with five or more ribosomes (large polysome fraction, LPS). Polysome loading was calculated as [(SPS + LPS)/(NPS + SPS + LPS)].
(B) Relative ribosome abundance, estimated from the total A_{254} signal. The results are the mean ± SD ($n \geq 5$).

Starch was degraded at a near constant rate throughout the night. This pattern was seen in all photoperiods, including the 18-h photoperiod when considerable amounts of starch remained at EN (Figure 5A). There may be a short delay until starch degradation commences at the start of the night, especially in the 4-, 6-, and 8-h photoperiods. This conclusion depends on a comparison of two values that differ only slightly, and is therefore sensitive to experimental noise. However, more detailed temporal analyses of starch and of maltose, which is a breakdown product of starch, in Pal et al. (2013) provide supporting evidence for a small delay before starch degradation commences.

Time-resolved changes of soluble metabolites are shown in Figure 5B–5D and Supplemental Figure 3. As already mentioned, the total amount of C in sugars was much lower than that in starch. As the photoperiod was lengthened, there was a slight increase in sucrose, glucose, and fructose at EN. Illumination led to an increase in sucrose (Figure 5B), glucose (Figure 5B), and fructose (Supplemental Table 3). The increase was most marked and rapid in short photoperiods, especially for glucose (Figure 5B), whereas it was strongly delayed in long photoperiods. In short photoperiods, accumulation of sugars coincides with rapid accumulation of starch at the start of the light period. In contrast, in long photoperiods, sugars accumulate towards the end of light period, when starch accumulation slows down.

At night, sucrose levels increased as the photoperiod was lengthened (Figure 5B). At a given photoperiod, however,

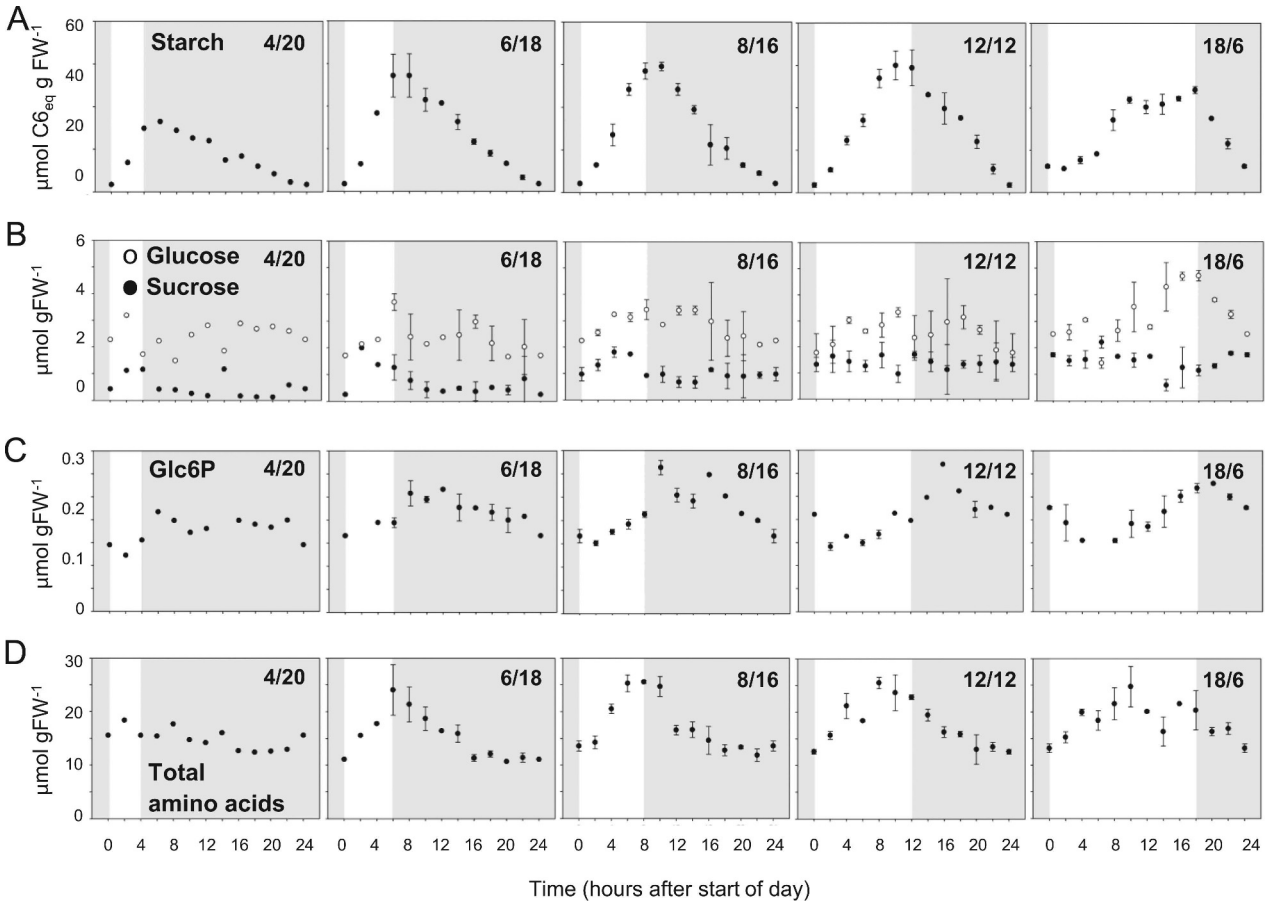

Figure 5. Diurnal Changes of Starch and Metabolites in a 4-, 6-, 8-, 12-, and 18-h Photoperiod.

(A) Starch.

(B) Sucrose and glucose.

(C) Glucose-6-phosphate.

(D) Total amino acids. Plots of fructose, malate and fumarate, are provided in Supplemental Figure 2, and the source data are provided in Supplemental Table 3. The plants were harvested at 21 d. The results are the mean ± SD (n = 2) except for the 4-h photoperiods where samples were combined for the analyses. Whilst it is not statistically valid to derive SD for two replicates, these values are given to provide an indication of the variation.

rather stable sucrose levels were found throughout the night. This mirrors the decrease in the rate of starch degradation as the photoperiod is shortened, and the constant rate of starch degradation throughout the night in a given photoperiod (Figure 5A). Glucose and fructose decreased at night in short photoperiods but were maintained at high levels in long photoperiods (Figure 5B).

Glucose 6-phosphate (Glc6P) is a key intermediate in carbohydrate synthesis, carbohydrate degradation, and glycolysis. Illumination led to a small decrease in Glc6P (Figure 5C). This is maybe surprising, as photosynthesis will lead to a large increase in the rate of Glc6P formation. A similar decrease was previously seen in spinach and barley (Stitt et al., 1985). This implies that use of Glc6P is stimulated in the light and may be partly due to light activation of sucrose phosphate synthase (SPS) (Huber and Huber, 1996; Stitt et al., 2010). The level of Glc6P in the first 2–4 h of the light period was similar in all photoperiods (Figure 5C), implying that the stimulation of starch accumulation in short photoperiods (Figure 5A) does not require an increase in Glc6P levels. Glc6P rose after darkening in all photoperiods, and was 20–40% higher in long photoperiods than in short photoperiods (Figure 5C).

The amount of C in organic acids and amino acids was much lower than that in starch (Supplemental Table 3). Amino acids rose in the light and decreased at night in a 6-, 8-, 12-, and 18-h photoperiod but showed no marked diurnal changes in the 4-h photoperiod (Figure 5D). Amino acids plateaued before the end of the light period in the 12-h and, especially, the 18-h photoperiod. This resembles the pattern of starch accumulation. Amino acid metabolism is interlinked with organic acid metabolism (Nunes-Nesi et al., 2010; Foyer and Zhang, 2011). Malate and fumarate rose in the light and decreased in the

first hours of the night (Supplemental Figure 3). These diurnal changes were small in a 4-h photoperiod, marked in a 6-, 8-, and 12-h photoperiod, and attenuated in an 18-h photoperiod, when the increase stopped by the middle of the light period, and the decrease at night was less marked.

Time-Resolved Modeling of Growth during the Diurnal Cycle

We investigated whether these time-resolved measurements of metabolites can be used to obtain more highly time-resolved estimates of growth. The summed C in starch, sugars, organic acids, and amino acids at each time point (Supplemental Table 3) was used to calculate the difference between adjacent time points (time interval t^i) (= ΔC). Growth rates in a given t^i were estimated as 'net photosynthesis in t^i – ΔC in $t^{i'}$' and 'ΔC in t^i – net respiration in $t^{i'}$', respectively (Supplemental Table 4). This calculation was performed for each of the 12 consecutive 2-h time intervals. These estimates often depend on small changes in starch and metabolite levels, and are sensitive to biological and technical noise. We therefore additionally used the individual values to calculate a moving average (see Supplemental Table 4). The individual estimates and moving averages were combined and used to fit second degree splines. Splines were separately fitted for the light period and the night. We did this because growth in the light is primarily dependent on C fixed in photosynthesis, whilst growth in the dark is primarily dependent on C provided by starch mobilization. The rate of growth at the end of the light period should therefore have no direct impact on growth in the first period of the night, and the rate of growth in the last period of the night should have no direct impact on growth in the first period of the light period.

The time-resolved estimates are shown in Figure 6. Estimated growth rates were generally high in the first 2 h of the light period. Rates were slightly lower in the 4- and 6-h photoperiods than in the 8- and 12-h photoperiods. This is due to increased allocation of C to starch and other metabolites in the first hours of the light period (see Table 2). In the 6-, 8-, and 12-h photoperiods growth decreased in the middle of the light period, and recovered later in the light period to higher rates than those at EN. The decline and recovery were delayed as the photoperiod was lengthened. Estimated growth rates decreased at the start of the night in the 4-, 6-, 8-, and 12-h photoperiods, and remained low in the 4- and 6-h photoperiods whilst there was a partial recovery in the 8- and 12-h photoperiods. Compared to shorter photoperiods, estimated growth rates in the 18-h photoperiod were low; this reflects the lower rate of photosynthesis per unit FW (Figure 1). They also showed a different temporal trend, with high rates immediately after illumination, a marked inhibition in mid-day, a recovery later in the light period to similar rates to those obtained early in the light period, and high rates during the night (Figure 6).

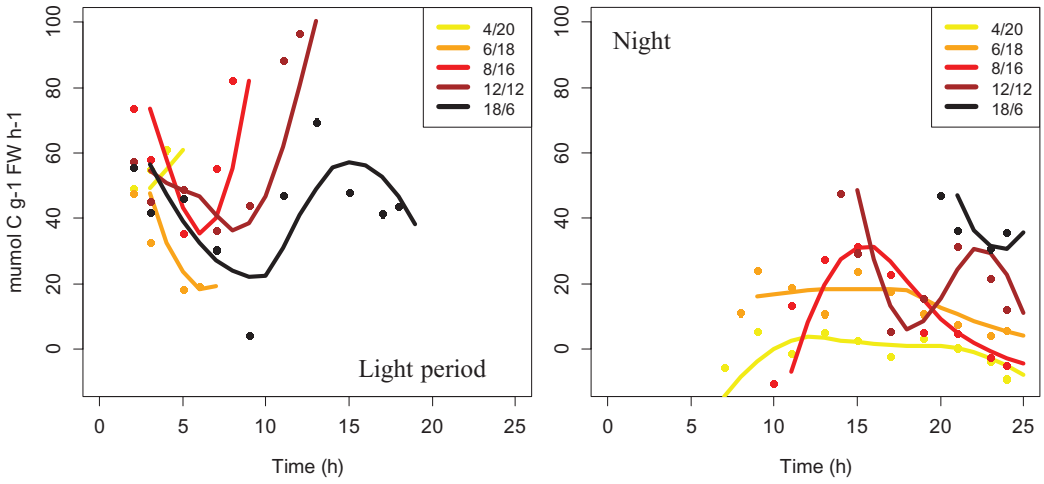

Figure 6. Time-Resolved Estimates of Growth during the Diurnal Cycle in Five Different Photoperiods.

The rates are estimated from the time-resolved data for metabolite levels collected at 2-h intervals throughout each photoperiod (Figure 3; see Supplemental Table 3 for source data and calculation of C atoms per metabolite) and the rates of photosynthesis and respiration in Figure 1, assuming the rates of photosynthesis and respiration do not change greatly during the light period and night, respectively. C in starch, sugars, organic acids, and amino acids was summed at each time point (see Supplemental Table 3) and the difference between the totals in adjacent time points (= ΔC). Growth rates in a time interval in the light and dark were calculated as 'A – ΔC' and 'ΔC– R', respectively, for each of the 12 consecutive 2-h time intervals. The modeled growth rates were used to compute moving averages between each consecutive pair of individual values. The individual values and moving averages were used to fit smooth curves using local polynomial regression of the second degree (loess splines). Splines were separately fitted to the growth rate estimates in the light period and the growth rates estimates in the night. To allow separate fitting of splines to the day and night growth estimates, moving averages were excluded that spanned dawn or dusk.

Table 2. Carbon Accumulated in Starch, Sugars, Organic Acids, and Amino Acids (as μmol C g^{-1} FW) and as Percent Assimilated Carbon) after 2- and 4-h Illumination of Plants Growing in a 4-, 6-, 8-, 12-, and 18-h Photoperiod.

Photoperiod	First 2 h in the light		First 4 h in the light	
	μmol C g^{-1} FW	% of fixed C	μmol C g^{-1} FW	% of fixed C
4/20	80	50	169	45
6/18	88	53	267	67
8/16	69	33	190	47
12/12	56	37	162	51
18/6	10	7	56	30

The data are from the experiment of Figures 4 and 5, and the source data are provide in Supplemental Table 3.

Profiling of Metabolic Intermediates at EN and ED

We used LC–MS/MS to analyze a further 42 metabolites in samples from the experiment of Figures 1–4, including phosphorylated intermediates, UDP-sugars, and more organic acids. The data are provided in Supplemental Table 1, and an overview of selected metabolites in Figure 7 and Supplemental Figure 3.

As already mentioned, sucrose increases as the photoperiod is lengthened, and is higher in the daytime than at night (Figure 2). Sucrose synthesis involves conversion of hexose phosphates and UDP-glucose to sucrose 6-P (Sucr6P) by SPS, followed by hydrolysis of Sucr6P by sucrose phosphatase. Increasing photoperiod length led to a progressive increase in Sucr6P and hexose phosphates (Figure 7). UDPGlc increased progressively in the light, whereas, in the dark, UDPGlc peaked in the 8-h photoperiod and then declined (Supplemental Figure 3). There was also a progressive increase in the sucrose-signal metabolite Tre6P as the photoperiod was lengthened, whereby Tre6P was always higher at ED than EN (Figure 7). The Calvin-Benson cycle and glycolytic metabolites 3PGA and PEP showed a progressive increase in the light, but plateaued in photoperiods above 8 h in the dark (Figure 7 and Supplemental Figure 3). Pyruvate and a large set of tricarboxyllic acid cycle intermediates including citrate, aconitate, isocitrate, 2-oxoglutarate, succinate, fumarate, and malate rose to a maximum in an 8-h photoperiod and decreased in longer photoperiods in both the light and the dark (Figure 7 and Supplemental Figure 3). While hexose phosphates appear to be closely linked to sucrose levels, the changes in UDP-glucose, 3PGA, PEP, and organic acids point to an additional input that promotes their use in long photoperiods, especially at night. This is consistent with the high growth rate in the night in long photoperiods.

Whilst pyruvate, malate, fumarate, and 2-oxoglutate are highest at ED, citrate, aconitate, and isocitrate are highest at EN. A reciprocal diurnal response of malate and citrate was reported in tobacco (Scheible et al., 1997, 2000). It has been proposed that malate and fumarate act as alternative C stores (Chia et al., 2000; Fahnenstich et al., 2007). However, their diurnal changes are partly compensated by reciprocal changes of other organic acids (Figure 7 and Supplemental Figure 3). It was recently shown that much of the 2-oxoglutarate that is synthesized to support N assimilation in the light is not derived from newly fixed C (Szecowka et al., 2013) but is instead formed from a preformed pool of citrate (Tcherkez et al., 2012a, 2012b).

Correlation Matrix for Metabolite Levels and the Rate of Growth in the Light and the Dark

The metabolite data and modeled rates of growth in the daytime and night were used to generate a correlation matrix (Supplemental Table 5). Two matrices were generated: one using data for all photoperiods and one excluding values for the 18-h photoperiod, where growth is not limited by C (see Figures 1 and 2 and the 'Discussion' section). Many biomass–metabolite pairs showed a high Pearson correlation (R_P) (Supplemental Figures 4 and 5). However, due to the large numbers of measured traits and relatively restricted number of treatments, most of these relations were not significant at a stringent false discovery rate (FDR). Table 3 summarizes metabolites that showed a significant correlation to growth. These include starch and shikimate in both matrices and sucrose, Tre6P, and total amino acids in the matrix that excluded the 18-h photoperiod treatment. The correlation with starch is likely to be secondary; longer days lead to increased A^D and increased growth in the day, and also to increased starch at ED that, in combination with a short night, will allow faster growth in the night. Figure 8 explores the relationship between growth, sucrose, and Tre6P, and Figure 9 explores the relationship between growth, amino acids, and shikimate. The plots distinguish between data points corresponding to the light period and the night, and identify the data point corresponding to the light period in the 18-h photoperiod.

Tre6P correlated with sucrose in the light and the dark, with a steeper slope in the light (Figure 8A). A correlation between sucrose and Tre6P has been reported previously (Lunn et al., 2006; Carillo et al., 2013; Nunes et al., 2013). Sucrose correlated with growth at night ($R_P = 0.99$) and in the light ($R_P = 0.96$, 18-h photoperiod data point is excluded) with a combined regression $R_P = 0.92$ for the light and the night

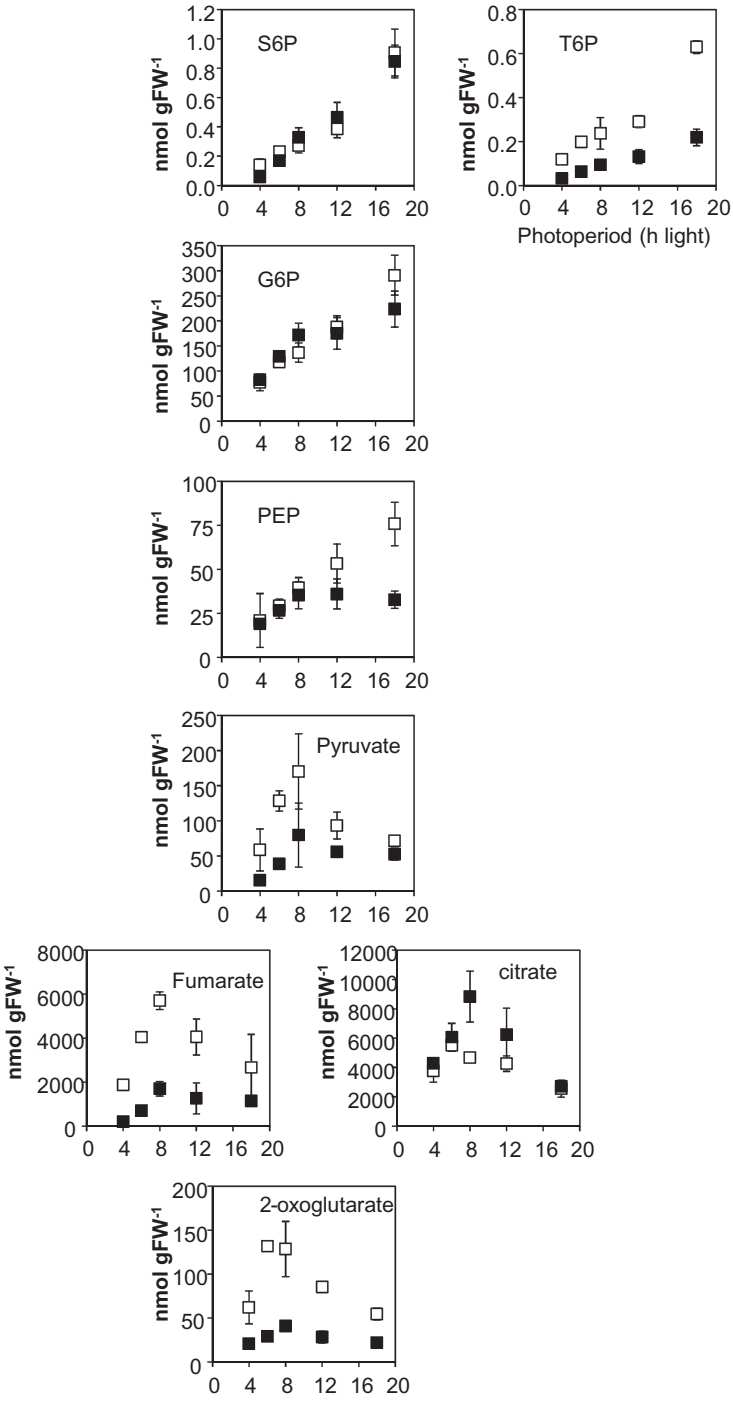

Figure 7. Selected Metabolic Intermediates in a 4-, 6-, 8-, 12-, and 18-h Photoperiod.

Data for ED (open symbols) and EN (closed symbols) are distinguished. Source data are provided in Supplemental Table 1; further plots are provided in Supplemental Figure 3. The results are the mean ± SD (n = 5).

(Figure 8B). Tre6P also correlated with growth in the dark (R_P = 0.99) and the light (R_P = 0.88, 18-h photoperiod point is excluded), with a similar slope at both times and a combined regression of R_P = 0.95 for the light and the dark (Figure 8C).

Amino acids (Figure 9A) and shikimate (Figure 9B) correlated with growth, with similar slopes in both the light and the dark. Shikimate correlated with total amino acids in both the light and the dark, with a similar slope at both times (Figure 9C). Shikimate also correlated with Tre6P in the light and the dark (Figure 9D).

Tre6P and shikimate occupied a central place in the metabolite correlation matrix. Both metabolites correlated

Table 3. Metabolites Showing a Significant Correlation with Both Daytime and Night Growth Rates.

Metabolic trait	All photoperiods		4-, 6-, 8-, and 12-h photoperiods	
	Pearsons R	FDR	Pearsons R	FDR
Rate of starch synthesis or degradation	0.92	0.065	0.95	0.096
Sucrose content	0.83	1	0.97	0.063
Tre6P content	0.64	1	0.96	0.049
Shikimate content	0.94	0.018	0.98	0.008
Total amino acid content	0.88	0.023	0.97	0.020

Two cases are shown; for all photoperiods, and for only the 4, 6, 8 and 12 h photoperiods. Growth was limited by C in these photoperiods, but not in the 18-h photoperiod (see Figure 1). Significance was determined by the Bonferoni test; FDR levels of 1%, 5%, and 30% are indicated in the table. Full correlation matrices are provided in Supplemental Table 5. Units are μmol C g^{-1} FW h^{-1} for starch synthesis and degradation, μmol g^{-1} FW for sucrose and total amino acid content, and nmol g^{-1} FW for Tre6P and shikimate content. Scatter plots of some of these relationships are provided in Figures 8 and 9, and Supplemental Figure 9.

with starch, sucrose, and amino acids, Tre6P also correlated with 3PGA, and shikimate also correlated with malate and fumarate. Further correlations emerged between amino acids, malate, and fumarate, between malate, fumarate, and pyruvate, and between F6P, UDPGlc, Gal6P, and Gly3P. Almost all correlations were positive, with the exception of nitrate, which correlated negatively with Sucr6P, and showed non-significant negative correlations with many other traits including growth (Supplemental Figures 4 and 5). There was a progressive decrease in nitrate, especially at ED, as the photoperiod lengthened. However, it is unlikely that nitrate limits growth as the highest levels of total amino acids are found in the 18-h photoperiod. Much of the starch is converted at night to sucrose for transport to support growth of younger leaves. There was a remarkable correlation between the rate of starch degradation or the rate of growth and the levels of sucrose, Sucr6P, and Tre6P at night (Supplemental Figure 6).

DISCUSSION

Earlier studies showed that the rate of starch synthesis increases and the rate of starch degradation decreases in short photoperiods (Stitt et al., 1978; Chatterton and Silvius, 1979, 1980; Smith and Stitt, 2007), pacing starch breakdown and avoiding a strong depletion of sucrose at night (Gibon et al., 2009). Whilst enzymic capacity for photosynthesis is maintained in short photoperiods, the enzymic capacity of pathways required for growth is decreased (Gibon et al., 2009). This partly explains how the decreased rate of starch degradation in short photoperiods is accompanied by a decreased consumption of C for growth. The current study adds information about photosynthesis, respiration, ribosome abundance, polysome loading, and metabolite levels. By applying pathway-based modeling approaches to this multilevel data set, we provide information about the C-efficiency of growth, the diurnal timing of growth, and trade-offs in the use of ribosomes in different photoperiods. We also use correlation analysis to identify metabolites that correlate with growth and may play a role in the underlying regulation network.

Efficiency of Growth in Different Photoperiods

In a 4-, 6-, 8-, and 12-h photoperiod starch is almost completely consumed at EN indicating that *Arabidopsis* is C-limited in these growth conditions (Figure 2A). In agreement, growth increased linearly with photoperiod length and net daily C gain, with similar C-conversion efficiencies being achieved over a five-fold change in the daily C supply (Figure 1). This underlines that C-allocation and growth are regulated by a very effective regulatory network.

This relationship breaks down in long photoperiods. Considerable amounts of starch remain at EN in an 18-h photoperiod (see also Hadrich et al., 2012) and biomass increases only slightly between a 12- and an 18-h photoperiod, showing that growth is no longer C-limited, whilst the C-conversion efficiency decreases by 40%. Our results point to two reasons for this decrease in C-conversion efficiency and growth. The first is incomplete turnover of starch (see also Rasse and Tocquin, 2006). Starch at EN in the 18-h photoperiod represents ~20% of the C fixed in 1 d in these conditions. With a RGR of 0.32, biomass doubles every 2.5 d. Maintaining this residual pool of starch therefore sequesters ~8% of the net photosynthesis from growth. The second is altered leaf morphology. In long photoperiods, leaves are up to 25% thicker (Supplemental Figure 1). This will lead to a corresponding decrease in leaf area, with the result that less light is intercepted per unit FW. In the light-limiting growth conditions used in our study, much of the light is probably absorbed in the upper part of the leaf and increasing leaf thickness will not increase absorption of incident light. Whole-plant photosynthesis will depend on increasing leaf area to maximize light interception. This morphological adjustment accounts for much of the decrease in photosynthesis and C-conversion efficiency and the attenuation of growth, in long photoperiods.

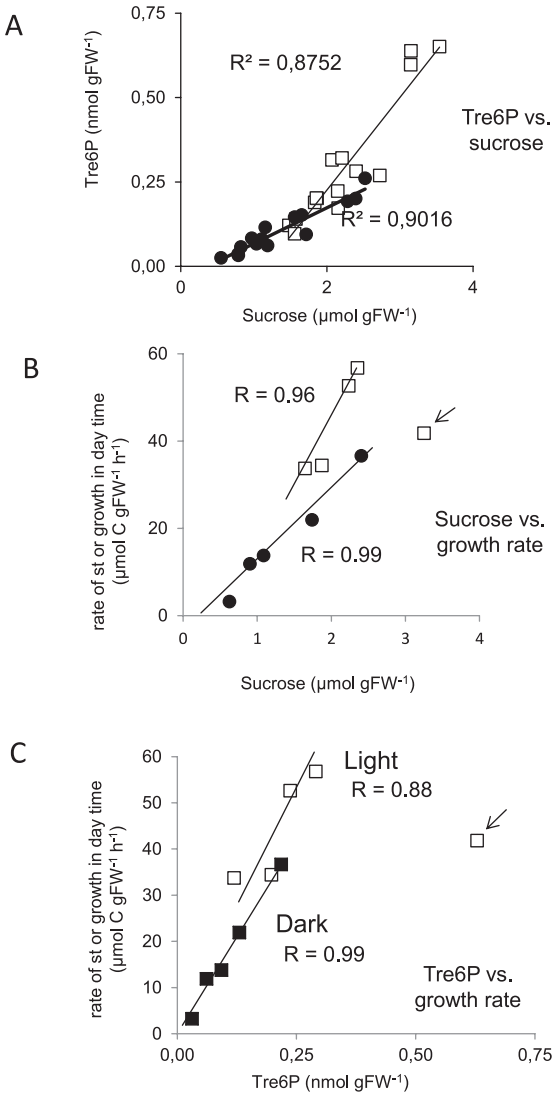

Figure 8. Correlations between Sucrose, Tre6P, and Growth.

(A) Sucrose versus Tre6P.

(B) Sucrose versus growth.

(C) Sucrose versus growth. Correlations for metabolite traits and growth in the daytime, and metabolite levels and growth at night are shown as open and closed symbols, respectively.

The regressions in plots (B) and (C) do not include the 18-h photoperiod ED data point (identified by an arrow). A full correlation matrix is provided in Supplemental Table 5

It is well established that leaves become thicker in high irradiance (Evans and Poorter, 2001; Terashima et al., 2001). This allows a higher capacity for photosynthesis per unit leaf area by increasing the area of mesophyll exposed to the gas phase (Terashima et al., 2001; Oguchi et al., 2003). There is genetic evidence that PHYB signaling contributes to these changes in leaf morphology (Lopez-Juez et al., 1998; Thiele et al., 1999; Boccalandro et al., 2009), possibly acting via an irradiance-sensing function (Casson et al., 2009; Poorter et al., 2009). However, the increase in leaf thickness in long photoperiods occurred at constant, and limiting, irradiance. Leaf morphology is largely determined by events that occur early in leaf development but responds to the light environment prevailing around mature leaves, leading to the hypothesis that a systemic signaling process is involved (Yano and Terashima, 2001; Thomas et al., 2004; Coupe et al., 2006). Sugars have been proposed as candidates for such signals (Kim et al., 2005; Coupe et al., 2006; Terashima et al., 2006). To prove this hypothesis, it will be necessary to develop strategies to manipulate *in planta* sugar levels without confounding effects due to changes in irradiance, water deficits, and nutrient supply.

Growth Occurs in the Day and Night, and the Distribution Is Flexible

Information about A, R, and metabolite levels were used to model the whole-plant C-balance and obtain estimates of growth, defined as the conversion of C into structural cellular components. Qualitatively similar results were obtained using a data set for metabolites at EN and ED that allowed estimation of average growth rates in the daytime and night (Figure 3), and a more detailed data set with metabolites measured every 2 h that allowed time-resolved estimates of growth (Figure 5). The growth rates in the night were then used to decompose R into R_g and R_m (Table 1).

Growth was flexibly distributed between the daytime and the night. The rate of growth in the daytime increased as the photoperiod was lengthened, reflecting the decreased allocation of C to temporary C-reserves in long photoperiods. The rate of growth in the night also increased as the photoperiod was lengthened, reflecting the increased amount of starch available at ED and the decreasing length of the night. As a result, the rate of growth at night was negligible in very short photoperiods, and comparable to the rate of growth in the daytime in long photoperiods. When the distribution of growth between the daytime and night is considered, in very short photoperiods, there was little growth at night, in a 6-h photoperiod over half the growth occurred at night and, in longer photoperiod, the proportion of growth that occurred in the night decreased again. The distribution of growth between the day and night also changed when plants are grown in different temperature regimes (Pyl et al., 2012). Time-resolved estimates of growth (Figure 6) revealed a transient depression of growth in the middle of the light period, and showed that the decrease of growth in the night occurs soon after darkening. Further studies with clock mutants will be needed to reveal whether the inhibition of growth in the middle of the light period is functionally related to the depression of growth in the middle of the T-cycle in hypocotyls, which is mediated via repression of *PIF* genes by the Evening Complex (Nusinow et al., 2011). The rapid decrease of growth at the start of the night and maintenance of growth for the remainder of the night is in agreement with the proposal that starch degradation is paced by the clock

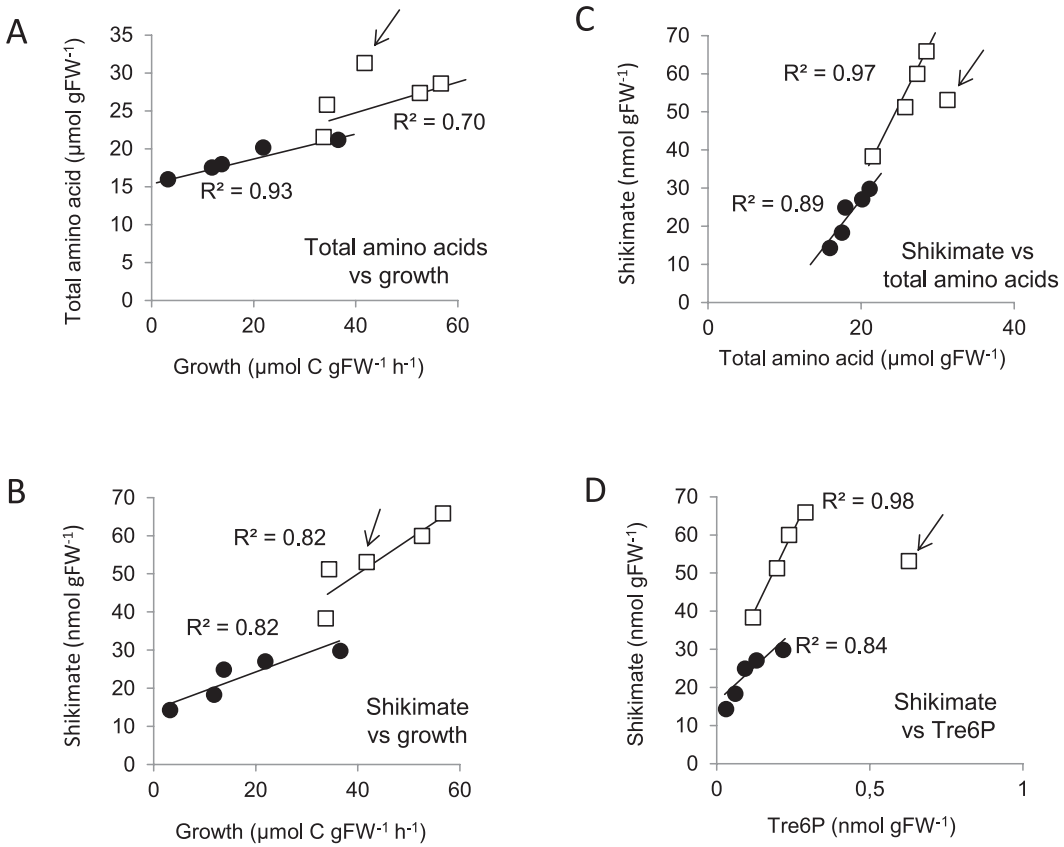

Figure 9. Correlations between Shikimate, Total Amino Acids, and Growth.

(A) Total amino acids versus growth.

(B) Shikimate versus growth.

(C) Total amino acids versus shikimate.

(D) Shikimate vs. Tre6P. Correlations for metabolite traits and growth in the daytime, and metabolite levels and growth at night are distinguished by open and closed symbols, respectively. The regressions do not include the 18-h ED data point photoperiod (identified by an arrow). A full correlation matrix is provided in Supplemental Table 5.

paces (Graf et al., 2010; Graf and Smith, 2011) and provides C throughout the night to support metabolism and growth (Stitt and Zeeman, 2012).

When *Arabidopsis* Col-0 is grown in a 12-h photoperiod at 160 µmol m^{-2} s^{-1} and 20°C, C starvation genes and catabolism of cell components are not induced during the night, but are induced after a 2–4-h extension of the night (Blasing et al., 2005; Usadel et al., 2008; Gibon et al., 2009). The question arises, what happens if there is insufficient starch to support the costs of maintenance at night? Modeled values for R_m were similar in all photoperiods; this may reflect the constant protein content. Thus, whilst only a small part of the starch is consumed for maintenance during long photoperiods, the proportion rises in short photoperiods and almost all the starch is used for maintenance in the 4-h photoperiod treatment. The photoperiod below which C reserves are insufficient to support growth at night will depend on factors that influence the rate of photosynthesis and starch accumulation (e.g. light intensity) and the rate of R_m at night (e.g. night temperature; Penning de Vries et al., 1979; Amthor, 2000). When *Arabidopsis* was grown in an 8-h photoperiod at 24°C, most of the starch was consumed for maintenance (Pyl et al., 2012). Recently, Izumi et al. (2013) reported that catabolism is induced in the night in *Arabidopsis* Col-0, which is in apparent contradiction to our studies (see above). However, their plants were grown at 24°C in a 10-h photoperiod with low light (100 µmol m^{-2} s^{-1}), and contained almost three-fold lower starch at ED (25 µmol Glc equivalents g^{-1} FW) than in our experiments. It is plausible that insufficient starch was accumulated to cover the requirements of maintenance.

Summarizing, this study and that of Pyl et al. (2012) uncover a remarkable flexibility in the diurnal timing of growth in *Arabidopsis* and show that the distribution is largely explained by the amount of starch that is available at ED, the length of the night, and the amount of C that is required for maintenance at night.

Optimization of Ribosome Use in Different Photoperiods

Large molecular machines are required to convert metabolites into cellular components like proteins, cell wall polymers, and

lipids. Protein synthesis represents a major component of cellular growth. Ribosomes account for up to 50% of the total cellular protein and 80% of the RNA in growing yeast cells, and ATP consumption during protein synthesis can account for a large part of total ATP turnover in a growing yeast cell (Warner, 1999; Rudra and Warner, 2004). We investigated the impact of photoperiod on ribosome abundance and polysome loading to provide insights into how the production and use of this molecular machinery are optimized in plants.

Ribosome abundance did not change between long and short photoperiods, even though growth rates decreased by up to five-fold. Ribosome loading into polysomes was similar in all photoperiods in the light, and was high at night in long photoperiods but decreased at night in short photoperiods (Figure 4). The changes in polysome loading qualitatively match the diurnal timing of growth (Figure 3). Sucrose correlates robustly with polysome loading during diurnal cycles in a 12-h photoperiod (Pal et al., 2013). It is possible that changes of sucrose contribute to the changes in polysome loading in different photoperiods.

The changes in polysome loading are smaller than the changes in growth. However, we recently performed direct measurement of the rate of protein synthesis, and showed that the decrease in polysome loading at night underestimates the extent to which protein synthesis is inhibited (Pal et al., 2013). Plastids represent half the ribosomes in an *Arabidopsis* rosette (Piques et al., 2009; Pal et al., 2013). At night, plastid protein synthesis is strongly decreased due to a slow rate of elongation and ribosome arrest (Marin-Navarro et al., 2007).

Protein synthesis involves direct and indirect costs. The direct costs include the energy required to synthesize amino acids, to activate amino acids, and to synthesize the peptide bond. In the light, ATP, NAD(P)H, and C are generated by photosynthesis, whereas at night they are generated by the catabolism of reserves like starch leading to loss of free energy (Penning de Vries, 1975; Amthor, 2010; Raven, 2012). Direct costs are therefore minimized by restricting protein synthesis to the light period. The indirect costs include the C, nitrogen, and phosphorus invested in ribosomes and the cost of synthesizing and maintaining ribosomes (Warner, 1999; Rudra and Warner, 2004). Indirect costs are minimized by using ribosomes all the time, as this minimizes the ribosome abundance that is required to achieve a given rate of protein synthesis per day. In short photoperiods, ribosomes are used more heavily in the daytime than the night. This is due to constraints set by the amount of starch at ED and the long night, which result in a low rate of starch degradation and low C-availability at night. High ribosome abundance will be required to rapidly use C and energy during the short light period, providing an explanation for why ribosome abundance does not decrease in short photoperiods. In long photoperiods, ribosomes are used throughout the day and night, and the resulting increase in direct costs at night can be covered by the increased availability, and even excess, of C.

Stimulation of Starch Synthesis in Short Photoperiods

Several mechanisms could contribute to the stimulation of starch accumulation in short photoperiods. First, the clock may act indirectly to increase starch synthesis in short photoperiods, by restricting starch degradation and growth in the preceding night. Whereas there is a pronounced lag before starch accumulation starts in long days, starch accumulation commences immediately after EN in short photoperiods (Figure 5; see also Hadrich et al., 2012). This rapid onset of starch accumulation coincides with an accumulation of sugars (Figure 5). This pattern is reminiscent of the response to a single extension of the night, which leads to an inhibition of growth and, after re-illumination, rapid accumulation of sugars and starch accumulation because there is a delay until growth recovers (Gibon et al., 2004). Starch breakdown, C-availability and growth at night are progressively decreased as the photoperiod is shortened (Figures 3 and 5). This may result in a slight attenuation of growth, sugar accumulation, and increased accumulation of starch in the first hours in the light. This contrasts with long photoperiods, where growth is high in the night and the start of the light period, and there is a strong lag until starch accumulation starts. Second, starch accumulation slows down before the end of the light period in long photoperiods (Figure 5). As this is accompanied by an increase in sucrose and other soluble metabolites, it is unlikely to be due to competition of growth for C. Further experiments will be needed to identify the reason for this slowdown, which might include a restriction on the total amount of starch that can be accumulated or initiation of starch degradation towards the end of the light period. Third, enzyme activity profiling revealed a progressive increase in the ratio of AGPase/SPS activity at EN as the photoperiod is shortened (Gibon et al., 2009; confirmed in the current experiments; see Supplemental Figure 7). These *in vitro* assays provide evidence for a progressive increase in the capacity for starch synthesis, relative to sucrose synthesis.

Network Analysis Reveals that Tre6P and Shikimate Correlate with Growth in C-Limited Conditions

Integration of the information on growth and starch turnover with the levels of over 40 metabolites revealed that many metabolites correlate with each other, and with starch turnover and growth (Supplemental Figures 4 and 5), showing that the photoperiod-dependent changes in starch turnover and growth are an output from a coordinated network.

Starch degradation correlated especially strongly with sucrose, Sucr6P, and Tre6P (Supplemental Figure 6) and growth in the daytime and night correlated strongly with the Tre6P (Figure 8). Tre6P is a sucrose signal (Lunn et al., 2006; Smeekens et al., 2010; Stitt et al., 2010; Carillo et al., 2013) and is implicated in the regulation of growth (Paul et al., 2010; Delatte et al., 2011; Nunes et al., 2013) and development (Schluepmann et al., 2003; Wahl et al., 2013). Tre6P has

been reported to inhibit SnRK1 (Zhang et al., 2009) and it has been proposed that this provides a pathway to promote protein synthesis and growth when sugars are high (Paul et al., 2010; Nunes et al., 2013). However, mutants with constitutively altered levels of Tre6P show complex and pleiotropic phenotypes (Schluepmann et al., 2003; Gomez et al., 2006; Stitt et al., 2010). There are many further sugar signaling pathways (Smeekens et al., 2010). Specific genetic interventions including cell-specific and inducible changes in Tre6P will be needed to elucidate the signaling pathways between Tre6P and growth. Growth also correlated with total amino acid levels and, more strongly, with shikimate (Figure 9). Shikimate is an intermediate in amino acid biosynthesis and may act as a read-out for amino acid biosynthesis. This idea is supported by the strong correlation between shikimate and total amino acids, although it should be noted that the latter will also be affected by the rate of use of amino acids for protein synthesis.

Concluding Remarks

These studies were restricted to vegetative growth. Changes can be expected in the way a plant manages its C reserves during reproductive growth. Following initiation, young leaves are initially a sink, whose growth must be supported by the remainder of the plant, but later act as a source of C for the remainder of the plant. In contrast, flowering and seed set result in the establishment of sinks whose net demand increases with time as the seed grows. Further studies are needed to learn how plants pace flower development and seed filling to avoid exceeding their C reserves. One possibility is that plants modify their C allocation to increase reserves prior to flowering. Another possibility is that flowering is regulated by C reserves. It was recently shown that the sucrose-signal Tre6P promotes flowering, acting via both the FT/CO photoperiod pathway and the maturity pathway (Wahl et al., 2013). This may tune the timing, and possibly the copiousness, of flowering to C availability. At a later stage in reproductive growth, it is well known that many stresses lead to flower and seed abortion, with resulting loss of yield in crop plants (Stevenson, 1981; Ruan et al., 2012). C starvation in *Arabidopsis* also leads to abortion of flowers and very young seeds, and cessation of growth of older siliques (Smith and Stitt, 2007). When C becomes available again, flowering and silique growth recommence. This might reflect a developmental switch to decrease initiation of new sinks during C-starvation, prioritizing survival of the reproductive meristem and use of resources that have already been invested in existing siliques. Finally, in many cases, the later stage of seed fill is accompanied by large-scale senescence and remobilization of resources from vegetative organs.

METHODS

Arabidopsis Col0 was grown in a 18-h/6-h, 12-h/12-h, 8-h/16-h, 6-h/18-h, and 4-h/20-h light/dark cycle (irradiance 160 μmol m^{-2}, 21°C and 19°C in the light and dark, respectively) (Gibon et al., 2009) and harvested after 30 d (five or six samples, each containing 15 rosettes) (Figures 1–4 and 7–9). For Figures 5 and 6, plants were grown from germination in the above photoperiods (temperature and irradiance as above) and harvested after 21 d (two replicates, 11–15, 25–30, and 70–90 rosettes per sample for 12–18-h, 6–8-h, and 4-h photoperiods, respectively. At harvest, whole rosettes were frozen in liquid nitrogen. Harvests at night were performed in the presence of low-intensity green lamp. Samples were homogenized and sub-aliquoted at –70°C using a cryorobot (Stitt et al., 2007b) and stored at –70°C. Chemicals were purchased as in Pyl et al. (2012). Starch, sucrose, glucose, fructose, malate, fumarate, glucose-6-phosphate, total amino acids, chlorophyll, and protein were measured via robotized assays (Cross et al., 2006; Nunes-Nesi et al., 2007; Pyl et al., 2012). Phosphorylated intermediates, Tre6P, and other organic acids were analyzed by reverse phase or anion exchange LC–MS/MS (Lunn et al., 2006; Arrivault et al., 2009). Polysome fractionation was as previously described (Pyl et al., 2012; Pal et al., 2013). Whole rosette gas exchange measurements were performed 1–2 d before harvest using the LI-6400XT portable photosynthesis system (LI-COR Biosciences) with a Whole Plant Arabidopsis Chamber with an RGB LED light source (Pyl et al., 2012). Photosynthesis was measured at the start of the light period and respiration at the EN on the day of harvest. All calculations were conducted using Excel or R software (R Development Core Team, 2008). Local polynomial regression splines were fitted using the loess function (R version 2.15.3).

SUPPLEMENTARY DATA

Supplementary Data are available at *Molecular Plant Online.*

FUNDING

This research was supported by the Max Planck Society and the European Commission FP7 collaborative project TiMet under contract no. 245143.

ACKNOWLEDGMENTS

This work was supported by the Max Planck Society, and the EU (collaborative project TiMet under contract no. 245143). We are indebted to Alison Smith, Andrew Millar, and Sam Zeeman for illuminating discussion. No conflict of interest declared.

REFERENCES

Amthor, J.S. (2000). The McCree-de Wit-Penning de Vries-Thornley respiration paradigms: 30 years later. Ann. Bot. **86**, 1–20.

Amthor, J.S. (2010). From sunlight to phytomass: on the potential efficiency of converting solar radiation to phyto-energy. New Phytol. **188**, 939–959.

Arrivault, S., Guenther, M., Ivakov, A., Feil, R., Vosloh, D., van Dongen, J.T., Sulpice, R., and Stitt, M. (2009). Use of reverse-phase liquid chromatography, linked to tandem mass spectrometry, to profile the Calvin cycle and other metabolic intermediates in *Arabidopsis* rosettes at different carbon dioxide concentrations. Plant J. **59**, 824–839.

Bailey-Serres, J. (1999). Selective translation of cytoplasmic mRNAs in plants. Trends Plant Sci. **4**, 142–148.

Barajas-Lopez, J.D.D., Serrato, A.J., Cazalis, R., Meyer, Y., Chueca, A., Reichheld, J.P., and Sahrawy, M. (2011). Circadian regulation of chloroplastic f and m thioredoxins through control of the CCA1 transcription factor. J. Exp. Bot. **62**, 2039–2051.

Blasing, O.E., Gibon, Y., Gunther, M., Hohne, M., Morcuende, R., Osuna, D., Thimm, O., Usadel, B., Scheible, W.R., and Stitt, M. (2005). Sugars and circadian regulation make major contributions to the global regulation of diurnal gene expression in *Arabidopsis*. Plant Cell. **17**, 3257–3281.

Boccalandro, H.E., Rugnone, M.L., Moreno, J.E., Ploschuk, E.L., Serna, L., Yanovsky, M.J., and Casal, J.J. (2009). Phytochrome B enhances photosynthesis at the expense of water-use efficiency in *Arabidopsis*. Plant Physiol. **150**, 1083–1092.

Carillo, P., Feil, R., Gibon, Y., Nagasawa, N.N., Jackson, D., Bläsing, O.E., Höhne, M., Stitt, M., and Lunn, J.E. (2013). A fluorimetric assay for trehalose in the picomole range. Plant Methods. **9**, 21.

Caspar, T., Huber, S.C., and Somerville, C. (1985). Alterations in growth, photosynthesis, and respiration in a starchless mutant of *Arabidopsis-thaliana* (L) deficient in chloroplast phosphoglucomutase activity. Plant Physiol. **79**, 11–17.

Casson, S.A., Franklin, K.A., Gray, J.E., Grierson, C.S., Whitelam, G.C., and Hetherington, A.M. (2009). Phytochrome B and PIF4 regulate stomatal development in response to light quantity. Curr. Biol. **19**, 229–234.

Chatterton, N.J., and Silvius, J.E. (1979). Photosynthate partitioning into starch in soybean leaves. 1. Effects of photoperiod versus photosynthetic period duration. Plant Physiol. **64**, 749–753.

Chatterton, N.J., and Silvius, J.E. (1980). Photosynthate partitioning into leaf starch as affected by daily photosynthetic period duration in 6 species. Physiol. Plant. **49**, 141–144.

Chia, D.W., Yoder, T.J., Reiter, W.D., and Gibson, S.I. (2000). Fumaric acid: an overlooked form of fixed carbon in *Arabidopsis* and other plant species. Planta. **211**, 743–751.

Chow, B.Y., and Kay, S.A. (2013). Global approaches for telling time: omics and the *Arabidopsis* circadian clock. Semin. Cell Dev. Biol. **24**, 383–392.

Coupe, S.A., et al. (2006). Systemic signalling of environmental cues in *Arabidopsis* leaves. J. Exp. Bot. **57**, 329–341.

Cross, J.M., von Korff, M., Altmann, T., Bartzetko, L., Sulpice, R., Gibon, Y., Palacios, N., and Stitt, M. (2006). Variation of enzyme activities and metabolite levels in 24 *Arabidopsis* accessions growing in carbon-limited conditions. Plant Physiol. **142**, 1574–1588.

Delatte, T.L., Sedijani, P., Kondou, Y., Matsui, M., de Jong, G.J., Somsen, G.W., Wiese-Klinkenberg, A., Primavesi, L.F., Paul, M.J., and Schluepmann, H. (2011). Growth arrest by trehalose-6-phosphate: an astonishing case of primary metabolite control over growth by way of the SnRK1 signaling pathway. Plant Physiol. **157**, 160–174.

Evans, J.R., and Poorter, H. (2001). Photosynthetic acclimation of plants to growth irradiance: the relative importance of specific leaf area and nitrogen partitioning in maximizing carbon gain. Plant Cell Environ. **24**, 755–767.

Fahnenstich, H., Saigo, M., Niessen, M., Zanor, M.I., Andreo, C.S., Fernie, A.R., Drincovich, M.F., Flugge, U.I., and Maurino, V.G. (2007). Alteration of organic acid metabolism in *Arabidopsis* overexpressing the maize C(4)NADP-malic enzyme causes accelerated senescence during extended darkness. Plant Physiol. **145**, 640–652.

Farre, E.M., and Weise, S.E. (2012). The interactions between the circadian clock and primary metabolism. Curr. Opin. Plant Biol. **15**, 293–300.

Foyer, C.H., and Zhang, H. (2011). Nitrogen Metabolism in Plants in the Post-Genomic Era (Chichester, West Sussex and Ames, Iowa: Wiley-Blackwell).

Geiger, D.R., and Servaites, J.C. (1994). Diurnal regulation of photosynthetic carbon metabolism in C-3 plants. Annu. Rev. Plant Physiol. Plant Mol. Biol. **45**, 235–256.

Gibon, Y., Blaesing, O.E., Palacios-Rojas, N., Pankovic, D., Hendriks, J.H., Fisahn, J., Hohne, M., Gunther, M., and Stitt, M. (2004). Adjustment of diurnal starch turnover to short days: depletion of sugar during the night leads to a temporary inhibition of carbohydrate utilization, accumulation of sugars and post-translational activation of ADP-glucose pyrophosphorylase in the following light period. Plant J. **39**, 847–862.

Gibon, Y., Pyl, E.T., Sulpice, R., Lunn, J.E., Hohne, M., Gunther, M., and Stitt, M. (2009). Adjustment of growth, starch turnover, protein content and central metabolism to a decrease of the carbon supply when *Arabidopsis* is grown in very short photoperiods. Plant Cell Environ. **32**, 859–874.

Gomez, L.D., Baud, S., Gilday, A., Li, Y., and Graham, I.A. (2006). Delayed embryo development in the ARABIDOPSIS TREHALOSE-6-PHOSPHATE SYNTHASE 1 mutant is associated with altered cell wall structure, decreased cell division and starch accumulation. Plant J. **46**, 69–84.

Graf, A., and Smith, A.M. (2011). Starch and the clock: the dark side of plant productivity. Trends Plant Sci. **16**, 169–175.

Graf, A., Schlereth, A., Stitt, M., and Smith, A.M. (2010). Circadian control of carbohydrate availability for growth in *Arabidopsis* plants at night. Proc. Natl Acad. Sci. U S A. **107**, 9458–9463.

Hadrich, N., et al. (2012). Mutagenesis of cysteine 81 prevents dimerization of the APS1 subunit of ADP-glucose pyrophosphorylase and alters diurnal starch turnover in *Arabidopsis thaliana* leaves. Plant J. **70**, 231–242.

Hendriks, J.H.M., Kolbe, A., Gibon, Y., Stitt, M., and Geigenberger, P. (2003). ADP-glucose pyrophosphorylase is activated by post-translational redox-modification in response to light and to sugars in leaves of *Arabidopsis* and other plant species. Plant Physiol. **133**, 838–849.

Huber, S.C., and Huber, J.L. (1996). Role and regulation of sucrose-phosphate synthase in higher plants. Annu. Rev. Plant Physiol. Plant Mol. Biol. **47**, 431–444.

Izumi, M., Hidema, J., Makino, A., and Ishida, H. (2013). Autophagy contributes to nighttime energy availability for growth in *Arabidopsis*. Plant Physiol. **161**, 1682–1693.

Kim, G.T., Yano, S., Kozuka, T., and Tsukaya, H. (2005). Photomorphogenesis of leaves: shade-avoidance and differentiation of sun and shade leaves. Photochem. Photobiol. Sci. **4**, 770–774.

Kolbe, A., Tiessen, A., Schluepmann, H., Paul, M., Ulrich, S., and Geigenberger, P. (2005). Trehalose 6-phosphate regulates starch synthesis via posttranslational redox activation of ADP-glucose pyrophosphorylase. Proc. Natl Acad. Sci. U S A. **102**, 11118–11123.

Lopez-Juez, E., Jarvis, R.P., Takeuchi, A., Page, A.M., and Chory, J. (1998). New *Arabidopsis* cue mutants suggest a close connection between plastid- and phytochrome regulation of nuclear gene expression. Plant Physiol. **118**, 803–815.

Lu, Y., Gehan, J.P., and Sharkey, T.D. (2005). Daylength and circadian effects on starch degradation and maltose metabolism. Plant Physiol. **138**, 2280–2291.

Lunn, J.E., Feil, R., Hendriks, J.H.M., Gibon, Y., Morcuende, R., Osuna, D., Scheible, W.R., Carillo, P., Hajirezaei, M.R., and Stitt, M. (2006). Sugar-induced increases in trehalose 6-phosphate are correlated with redox activation of ADPglucose pyrophosphorylase and higher rates of starch synthesis in *Arabidopsis thaliana*. Biochem. J. **397**, 139–148.

Marin-Navarro, J., Manuell, A.L., Wu, J., and Mayfield, S.P. (2007). Chloroplast translation regulation. Photosynthesis Res. **94**, 359–374.

Michalska, J., Zauber, H., Buchanan, B.B., Cejudo, F.J., and Geigenberger, P. (2009). NTRC links built-in thioredoxin to light and sucrose in regulating starch synthesis in chloroplasts and amyloplasts. Proc. Natl Acad. Sci. U S A. **106**, 9908–9913.

Nunes, C., O'Hara, L.E., Primavesi L.F., Delatte, T.L., Schluepmamm, H., Somsen, G.W., Silva, A.B., Fevereiro, P.S., Wingler, A., and Paul, M. (2007). The trehalose 6-phosphate/SnRK1 signaling pathway primes growth recovery following relief of sink limitation. Plant Physiol. **162**, 1720–1732.

Nunes, C., O'Hara, L.E., Primavesi, L.F., Delatte, T.L., Schluepmann, H., Somsen, G.W., Silva, A.B., Fevereiro, P.S., Wingler, A., and Paul, M.J. (2013). The trehalose 6-phosphate/SnRK1 signaling pathway primes growth recovery following relief of sink limitation. Plant Physiol. **162**, 1720–1732.

Nunes-Nesi, A., Carrari, F., Gibon, Y., Sulpice, R., Lytovchenko, A., Fisahn, J., Graham, J., Ratcliffe, R.G., Sweetlove, L.J., and Fernie, A.R. (2007). Deficiency of mitochondrial fumarase activity in tomato plants impairs photosynthesis via an effect on stomatal function. Plant J. **50**, 1093–1106.

Nunes-Nesi, A., Fernie, A.R., and Stitt, M. (2010). Metabolic and signaling aspects underpinning the regulation of plant carbon nitrogen interactions. Mol. Plant. **3**, 973–996.

Nusinow, D.A., Helfer, A., Hamilton, E.E., King, J.J., Imaizumi, T., Schultz, T.F., Farre, E.M., and Kay, S.A. (2011). The ELF4–ELF3–LUX complex links the circadian clock to diurnal control of hypocotyl growth. Nature. **475**, 398–402.

Oguchi, R., Hikosaka, K., and Hirose, T. (2003). Does the photosynthetic light-acclimation need change in leaf anatomy? Plant Cell Environ. **26**, 505–512.

Pal, S.K., Liput, M., Piques, M., Ishihara, H., Obata, T., Martins, M.C., Sulpice, R., van Dongen, J.T., Fernie, A.R., Yadav, U.P., et al. (2013). Diurnal changes of polysome loading track sucrose content in the rosette of wild-type *Arabidopsis* and the starchless pgm mutant. Plant Physiol. **162**, 1246–1265.

Paul, M.J., Jhurreea, D., Zhang, Y., Primavesi, L.F., Delatte, T., Schluepmann, H., and Wingler, A. (2010). Upregulation of biosynthetic processes associated with growth by trehalose 6-phosphate. Plant Signaling & Behavior. **5**, 386–392.

Penning de Vries, F.W., Brunstin, A.H., and Vanlaar, H.H. (1974). Products, requirements and efficiency of biosynthesis—quantitative approach. J. Theor. Biol. **45**, 339–377.

Penning de Vries, F.W.T. (1975). Cost of maintenance processes in plant cells. Ann. Bot. **39**, 77–92.

Penning de Vries, F.W.T., Witlage, J.M., and Kremer, D. (1979). Rates of respiration and of increase in structural dry-matter in young wheat, ryegrass and maize plants in relation to temperature, to water-stress and to their sugar content. Ann. Bot. **44**, 595–609.

Piques, M., Schulze, W.X., Höhne, M., Usadel, B., Gibon, Y., Rohwer, J., and Stitt, M. (2009). Ribosome and transcript copy numbers, polysome occupancy and enzyme dynamics in *Arabidopsis*. Mol. Syst. Biol., 10.1038/msb.2009.1068.

Poire, R., Wiese-Klinkenberg, A., Parent, B., Mielewczik, M., Schurr, U., Tardieu, F., and Walter, A. (2010). Diel time-courses of leaf growth in monocot and dicot species: endogenous rhythms and temperature effects. J. Exp. Bot. **61**, 1751–1759.

Poorter, H., Walter, A., Fiorani, F., Schurr, U., and Niinemets, U. (2009). Meta-phenomics: building a unified framework for interpreting plant growth responses to diverse environmental variables. In Annual Meeting of the Society for Experimental Biology, Glasgow, Scotland, p. S224.

Pyl, E.T., Piques, M., Ivakov, A., Schulze, W., Ishihara, H., Stitt, M., and Sulpice, R. (2012). Metabolism and growth in *Arabidopsis* depend on the daytime temperature but are temperature-compensated against cool nights. Plant Cell. **24**, 2443–2469.

R Development Core Team (2008). R: A Language and Environment for Statistical Computing (Vienna: R Foundation for Statistical Computing).

Rasse, D.P., and Tocquin, P. (2006). Leaf carbohydrate controls over *Arabidopsis* growth and response to elevated CO2: an experimentally based model. New Phytol. **172**, 500–513.

Raven, J.A. (2012). Protein turnover and plant RNA and phosphorus requirements in relation to nitrogen fixation. Plant Sci. **190**, 25–5.

Ruan, Y.L., Patrick, J.W., Bouzayen, M., Osorio, S., and Fernie, A.R. (2012). Molecular regulation of seed and fruit set. Trends Plant Sci. **17**, 656–665.

Rudra, D., and Warner, J.R. (2004). What better measure than ribosome synthesis? Genes Dev. **18**, 2431–2436.

Scheible, W.R., GonzalezFontes, A., Lauerer, M., MullerRober, B., Caboche, M., and Stitt, M. (1997). Nitrate acts as a signal to induce organic acid metabolism and repress starch metabolism in tobacco. Plant Cell. **9**, 783–798.

Scheible, W.R., Krapp, A., and Stitt, M. (2000). Reciprocal diurnal changes of phosphoenolpyruvate carboxylase expression and cytosolic pyruvate kinase, citrate synthase and NADP-isocitrate dehydrogenase expression regulate organic acid metabolism during nitrate assimilation in tobacco leaves. Plant Cell Environ. **23**, 1155–1167.

Schluepmann, H., Pellny, T., van Dijken, A., Smeekens, S., and Paul, M. (2003). Trehalose 6-phosphate is indispensable for

carbohydrate utilization and growth in *Arabidopsis thaliana*. Proc. Natl Acad. Sci. U S A. **100**, 6849–6854.

Scialdone, A., Mugford, S.T., Feike, D., Skeffington, A., Borrill, P., Graf, A., Smith, A.M., and Howard, M. (2013). *Arabidopsis* plants perform arithmetic division to prevent starvation at night. eLife. **2**, e00669.

Smeekens, S., Ma, J.K., Hanson, J., and Rolland, F. (2010). Sugar signals and molecular networks controlling plant growth. Curr. Opin. Plant Biol. **13**, 274–279.

Smith, A.M., and Stitt, M. (2007). Coordination of carbon supply and plant growth. Plant Cell Environ. **30**, 1126–1149.

Stevenson, A.G. (1981). Flower and fruit abortion: proximate casues and ultimate function. Annu. Rev. Ecol. Syst. **12**, 253–279.

Stitt, M., and Zeeman, S.C. (2012). Starch turnover: pathways, regulation and role in growth. Curr. Opin. Plant Biol. **15**, 282–292.

Stitt, M., Bulpin, P.V., and Rees, T.A. (1978). Pathway of starch breakdown in photosynthetic tissues of *Pisum sativum*. Biochim. Biophys. Acta. **544**, 200–214.

Stitt, M., Gibon, Y., Lunn, J.E., and Piques, M. (2007a). Multilevel genomics analysis of carbon signalling during low carbon availability: coordinating the supply and utilisation of carbon in a fluctuating environment. Funct. Plant Biol. **34**, 526–549.

Stitt, M., Lunn, J., and Usadel, B. (2010). *Arabidopsis* and primary photosynthetic metabolism—more than the icing on the cake. Plant J. **61**, 1067–1091.

Stitt, M., Sulpice, R., Gibon, Y., Whitwell, A., Skilbeck, R., Parker, S., and Ellison, R. (2007b). Cryogenic grinder system. Patent No. 08146.0025U1, Germany.

Stitt, M., Wirtz, W., Gerhardt, R., Heldt, H.W., Spencer, C., Walker, D., and Foyer, C. (1985). A comparative study of metabolite levels in plant leaf material in the dark. Planta. **166**, 354–364.

Szecowka, M., Heise, R., Tohge, T., Nunes-Nesi, A., Vosloh, D., Huege, J., Feil, R., Lunn, J., Nikoloski, Z., Stitt, M., et al. (2013). Metabolic fluxes in an illuminated *Arabidopsis* rosette. Plant Cell. **25**, 694–714.

Tcherkez, G., Boex-Fontvieille, E., Mahe, A., and Hodges, M. (2012a). Respiratory carbon fluxes in leaves. Curr. Opin. Plant Biol. **15**, 308–314.

Tcherkez, G., Mahe, A., Guerard, F., Boex-Fontvieille, E.R.A., Gout, E., Lamothe, M., Barbour, M.M., and Bligny, R. (2012b). Short-term effects of CO2 and O2 on citrate metabolism in illuminated leaves. Plant Cell Environ. **35**, 2208–2220.

Terashima, I., Miyazawa, S.I., and Hanba, Y.T. (2001). Why are sun leaves thicker than shade leaves? Consideration based on analyses of CO2 diffusion in the leaf. J. Plant Res. **114**, 93–105.

Terashima, I., Sone, K., and Noguchi, K. (2006). Estimation of net CO_2 absorption rates by forest trees. Plant Cell Physiol. **47**, S5–S5.

Thiele, A., Herold, M., Lenk, I., Quail, P.H., and Gatz, C. (1999). Heterologous expression of *Arabidopsis* phytochrome B in transgenic potato influences photosynthetic performance and tuber development. Plant Physiol. **120**, 73–81.

Thomas, P.W., Woodward, F.I., and Quick, W.P. (2004). Systemic irradiance signalling in tobacco. New Phytol. **161**, 193–198.

Tiessen, A., Hendriks, J.H.M., Stitt, M., Branscheid, A., Gibon, Y., Farre, E.M., and Geigenberger, P. (2002). Starch synthesis in potato tubers is regulated by post-translational redox modification of ADP-glucose pyrophosphorylase: a novel regulatory mechanism linking starch synthesis to the sucrose supply. Plant Cell. **14**, 2191–2213.

Troein, C., Locke, J.C.W., Turner, M.S., and Millar, A.J. (2009). Weather and seasons together demand complex biological clocks. Curr. Biol. **19**, 1961–1964.

Usadel, B., Blasing, O.E., Gibon, Y., Retzlaff, K., Hoehne, M., Gunther, M., and Stitt, M. (2008). Global transcript levels respond to small changes of the carbon status during progressive exhaustion of carbohydrates in *Arabidopsis* rosettes. Plant Physiol. **146**, 1834–1861.

Wahl, V., Ponnu, J., Schlereth, A., Arrivault, S., Langenecker, T., Franke, A., Feil, R., Lunn, J.E., Stitt, M., and Schmid, M. (2013). Regulation of flowering by trehalose-6-phosphate signaling in *Arabidopsis thaliana*. Science. **339**, 704–707.

Walter, A., Silk, W.K., and Schurr, U. (2009). Environmental effects on spatial and temporal patterns of leaf and root growth. Annu. Rev. Plant Biol. **60**, 279–304.

Warner, J.R. (1999). The economics of ribosome biosynthesis in yeast. Trends Biochem. Sci. **24**, 437–440.

Wiese, A., Christ, M.M., Virnich, O., Schurr, U., and Walter, A. (2007). Spatio-temporal leaf growth patterns of *Arabidopsis thaliana* and evidence for sugar control of the diel leaf growth cycle. New Phytol. **174**, 752–761.

Yano, S., and Terashima, I. (2001). Separate localization of light signal perception for sun or shade type chloroplast and palisade tissue differentiation in *Chenopodium album*. Plant Cell Physiol. **42**, 1303–1310.

Yazdanbakhsh, N., Sulpice, R., Graf, A., Stitt, M., and Fisahn, J. (2011). Circadian control of root elongation and C partitioning in *Arabidopsis thaliana*. Plant Cell Environ. **34**, 877–894.

Zeeman, S.C., Kossmann, J., and Smith, A.M. (2010). Starch: its metabolism, evolution, and biotechnological modification in plants. Annu. Rev. Plant Biol. **61**, 209–234.

Zhang, Y.H., Primavesi, L.F., Jhurreea, D., Andralojc, P.J., Mitchell, R.A.C., Powers, S.J., Schluepmann, H., Delatte, T., Wingler, A., and Paul, M.J. (2009). Inhibition of SNF1-related protein kinase1 activity and regulation of metabolic pathways by trehalose-6-phosphate. Plant Physiol. **149**, 1860–1871.